Figure S1

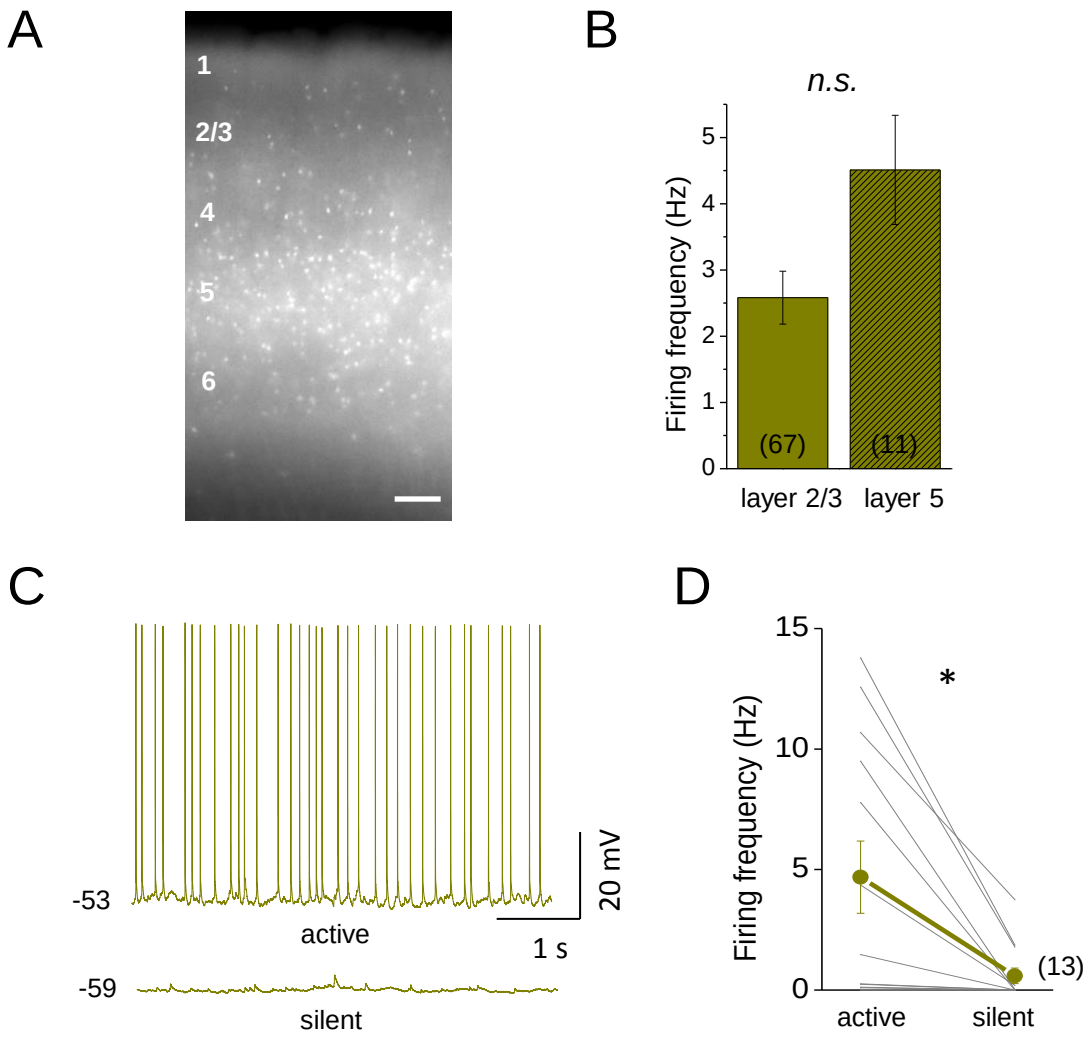

Figure S1. Spontaneous firing of a Sst cell *in vitro* is regulated by bath composition. (**A**) Laminar distribution pattern of Tdt+ cells in the barrel cortex in an acute brain slice from an Sst-IRES Cre x Ai14 (floxed Tdt) transgenic mouse. Scale bar: 100 μm (**B**) Spontaneous firing activity of Sst neurons under mACSF/active conditions across layers. (**C**) High spontaneous firing activity of L2/3 Sst cells under mACSF/active conditions (top traces) is suppressed following bath application of rACSF/silent conditions. (**D**) Within-cell comparisons of spontaneous layer 2/3 Sst cells firing between active and silent conditions. *p=0.008, paired t-test. Figure S1 is related to Figure 1.

Figure S2

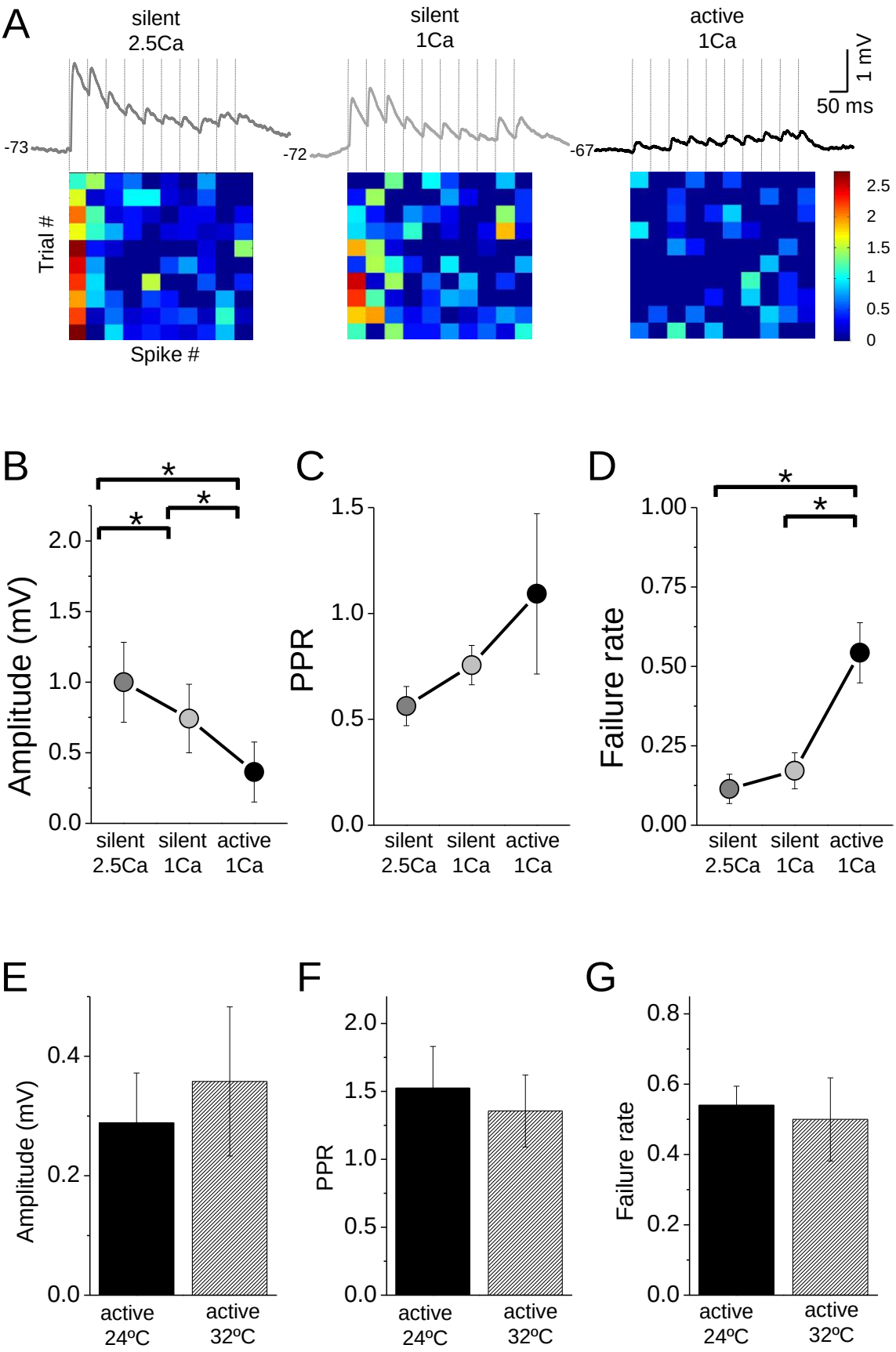
A
silent
2.5Ca
silent
1Ca
active
1Ca
1 mV
50 ms
-73
-72
-67
Trial #
Spike #
2.5
2
1.5
1
0.5
0
B
Amplitude (mV)
2.0
1.5
1.0
0.5
0.0
silent
2.5Ca
silent
1Ca
active
1Ca
C
PPR
1.5
1.0
0.5
0.0
D
Failure rate
1.00
0.75
0.50
0.25
0.00
E
Amplitude (mV)
0.4
0.2
0.0
active
24ºC
active
32ºC
F
PPR
2.0
1.5
1.0
0.5
0.0
G
Failure rate
0.8
0.6
0.4
0.2
0.0

Figure S2. The control of EPSP efficacy by extracellular Ca^{2+} levels and recording temperature. (**A**) Example connection recorded sequentially under 3 conditions: dark gray trace, rACSF/silent (2.5 mM $CaCl_2$ and 2.5 mM KCl); light gray trace, rACSF/low Ca^{2+} (1 mM $CaCl_2$ and 2.5 mM KCl) and black trace, mACSF/active (1 mM $CaCl_2$ and 3.5 mM KCl). Each trace is an average of 10 trials. Heatmap at bottom shows response amplitudes for 10 individual trials consisting of 10-spike responses every, using a linear scale where red is the maximum amplitude. (**B**) Mean amplitude of the first EPSP for cells recorded under all three conditions. (**C)** Comparison of PPR (EPSP amplitude of response 2/response 1) for individual cells recorded under all three conditions. (**D**) Comparison of failure rate for the first EPSP across cells recorded under all three conditions. n=7 cells for (C-D), *p<0.05 ANOVA. Note that only failure rate was significantly different according to the composition of the bath solution. (**E**) Comparison of failure rate for the first EPSP recorded under different temperatures: 24º (n=20) or 32ºC (n=6). (**F**) As in (E) but for PPR. (**G**) As in (E) but for failure rate. Figure S2 is related to Figure 2.

Figure S3

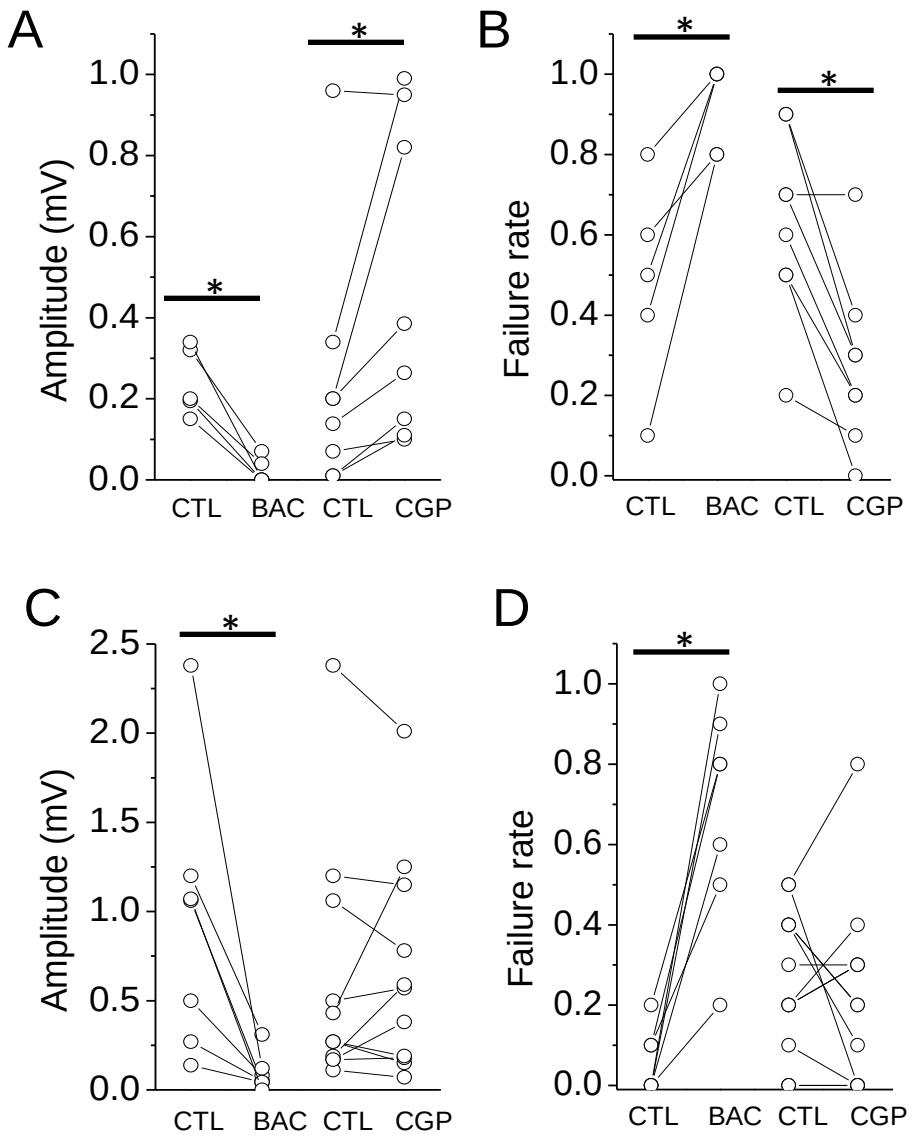

Figure S3. GABAb receptors do not affect basal excitatory transmission under silent network conditions. Within-cell comparisons of EPSP properties after GABAb modulation in active versus silent networks. (**A)** In active networks, baclofen significantly reduces EPSP amplitude (n=5 cells) and CGP significantly increases EPSP amplitude compared to baseline responses (n=8 cell, different from baclofen group). (**B**) As in (A) but for failure rate. (**C)** In silent networks, baclofen significantly reduces EPSP amplitude (n=7), but CGP has no effect (n=11). This indicates that basal activation of presynaptic GABAb receptors is negligible in silent networks. (**D)** As in (C) but for failure rate. *p<0.05 by paired t-test. Figure S3 is related to Figure 4.

Figure S4

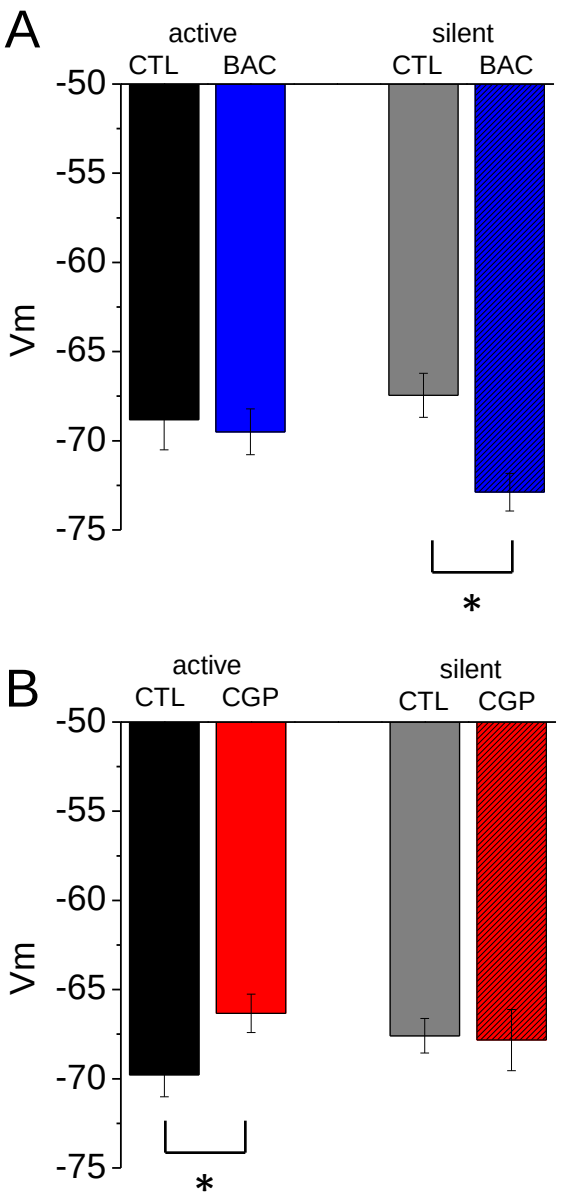

Figure S4. Postsynaptic effects of GABAb pharmacological manipulations. (**A**) Baclofen activation of GABAb receptors does not change Vrest in neurons under active network conditions (n=10), but does hyperpolarize neurons under silent network conditions (n=15). (**B**) GABAb blockade with CGP significantly depolarizes neurons during active network conditions (n=15), but has no effect on Vrest in neurons under silent network conditions (n=20). *p<0.05 paired t-test. Figure S4 is related to Figure 4.

Figure S5

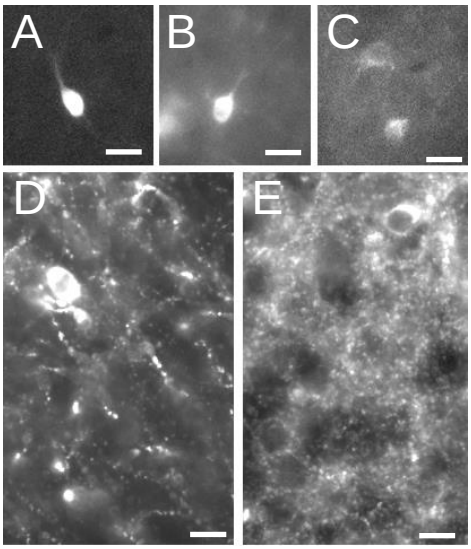
A
B
C
D
E

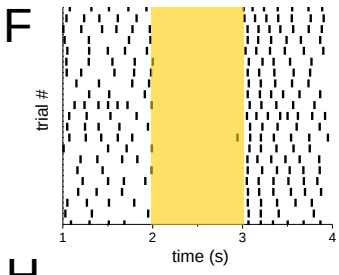
F
trial #
1
2
3
4
time (s)

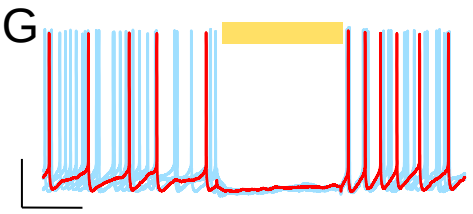
G

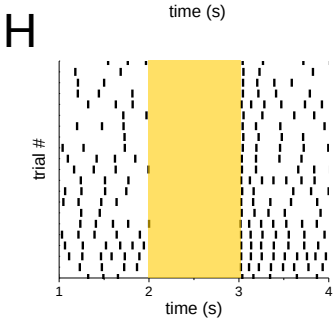
H
trial #
1
2
3
4
time (s)

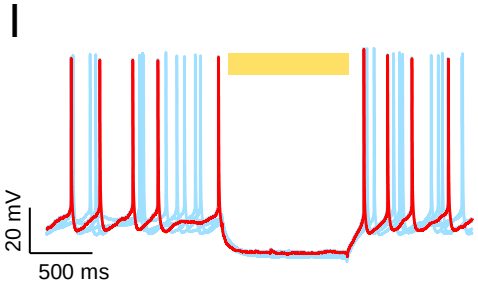
I
20 mV
500 ms

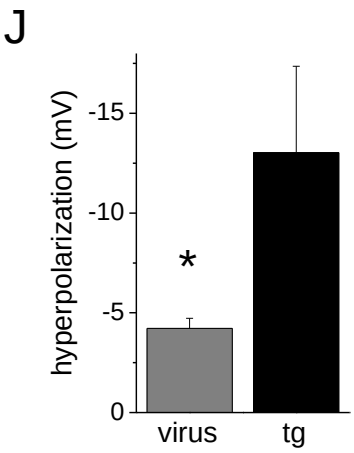
J
hyperpolarization (mV)
-15
-10
-5
0
*
virus
tg

Figure S5. Yellow-green light illumination hyperpolarizes Sst neurons and suppresses spontaneous firing. Sst-neuron labeling in L2/3 in Sst-IRES-Cre transgenic mice**.** (**A**) Example labeled cell from an acute brain slice taken from an Sst-IRES Cre x Ai14 (floxed Tdt) transgenic mouse. (**B)** Example labeled cell from an acute brain slice taken from an Sst-IRES Cre mice injected into S1 with AAV-virus containing a floxed Archaerhodopsin tagged with GFP. (**C)** Example labeled cell from Sst-Cre x Ai35 (floxed Arch tagged with GFP) transgenic mouse. Note that fluorescence signal from the transgenically-expressed Arch appears lower than in (B), although mean light-induced hyperpolarization was significantly greater (see J). Scale bar 20 μm. (**D**) Anti-GFP immunofluorescence in L2/3 from virally transduced animals. (**E**) Anti-GFP immunofluorescence in L2/3 from Sst-Cre x Ai35 transgenic mice. Scale bar 20 μm. (**F**) Spike raster plot for example Sst neuron, where recordings were guided by fluorescence labeling from expression of virally-transduced Arch-YFP transgene. Silencing of spontaneous activity during 1 s illumination (amber area) was reversed following the end of the light pulse. (**G)** Whole-cell current clamp recording showing 5 example sweeps (blue) during Sst silencing (amber bar indicates illumination) with a single trial shown in red. (**H)** As in (F), but for a Sst neuron from transgenic mouse expressing Arch in Sst cells. (**I**) As in (G), but for a Sst cell from a transgenic mouse. (**J**) Mean hyperpolarization induced by illumination for virally-transduced (n=9) or transgenic Arch expression (n=4) measured 500 ms after the onset of 1-s illumination. *$p<0.05$ by unpaired t-test. Figure S5 is related to Figure 5.

Table S1

Table S1. Ionic composition of extracellular solutions *in vivo* and *in vitro* (in mM)

ion	*Human**	*Rat**	*rACSF*	*mACSF^*
Na^+	147	152	119	119
K^+	2.9	3.4	2.5	3.5
Ca^{2+} (free)	1.0	1.0	2.5	1.0
Mg^{2+} (free)	0.7	0.88	1.3	0.5

*Somjen, 2004
^Maffei et al, 2004

Table S2

Table S2. Input resistance (R_i) and resting membrane potential V_{rest} in different ACSF compositions (mean±sem).

N=14 cells	silent 2.5 Ca^{2+}	silent 1 Ca^{2+}	active 1 Ca^{2+}
R_i (MΩ)	381.7±47.0	363.9±52.9	281.8± 45.8*
V_{rest} (mV)	-68.2±1.2	-67.6±1.9	-65.4±1.0

** p=0.01 paired t-test vs both silent condition values*

Supplemental Experimental Procedures

Animals

All experimental procedures were conducted in accordance with the National Institute of Health guidelines and were approved by the Institutional Animal Care and Use at Carnegie Mellon University.

The following strains of mice were used in these experiments: 1) wild-type C57Bl6 mice (Harlan); 2) Sst-IRES-Cre mice on a C57Bl6 background (Jackson Labs stock # 013044); 3) Pvalb-2A-Cre on a C57Bl6 background (Jackson Labs stock #012358) 4) Ai14 mice on a mixed background, C57Bl6J and B6;129S6 (Jackson Labs stock #007908) and 5) Ai35D on a C57Bl6 background (Jackson Labs stock # 012735).

Brain slice preparation

Experiments were performed in mice aged P12–P21, where P0 indicates the day of birth. Brain slices (350 μm thick) were prepared by an "across-row" protocol in which the anterior end of the brain was cut along a 45° plane toward the midline [S1]. Slices were recovered and maintained at 24° C in regular artificial cerebrospinal fluid (ACSF) composed of (in mM): 119 NaCl, 2.5 KCl, 2 $MgSO_4$, 2 $CaCl_2$, 1 NaH_2PO_4, 26.2 $NaHCO_3$, 11 glucose equilibrated with 95/5% O_2/CO_2

Whole-cell recording

Somata of layer 2 neurons in primary somatosensory cortex were targeted for whole-cell recording with borosilicate glass electrodes, resistance 4-8 MΩ. Electrode internal solution was composed of (in mM): 125 potassium gluconate, 2 KCl, 10 HEPES, 0.5 EGTA, 4 MgATP, and 0.3 NaGTP, at pH 7.25-7.35, 290 mOsm and contained trace amounts of Alexa 568 or 488 to verify the location of the recorded cell. Because of the difficulty in identifying connected pairs, the majority of recordings were carried out at room temperature (24°C) to enable longer recording periods, since prolonged incubation at warmer temperatures degrades cell health and recording quality. To block GABAa receptors 500 μM 4,40-dinitrostilbene-2,20-disulfonic acid, disodium salt (DNDS: Sigma) was added to the internal solution [S2]. Synaptically connected cells were identified by sequential paired-cell recordings, where cells were targeted based on pyramidal morphology and the distance between them was no longer than 100μm. The distance from the pia was typically between 200-250 μm. Recordings were performed in 3 ACSF solutions that differed only by concentrations of Mg^{2+}, Ca^{2+}, and K^+. Ionic concentrations were as follows (in mM): mACSF – 0.5 $MgSO_4$, 1 $CaCl_2$, 3.5 KCl; rACSF – 1.3 $MgSO_4$, 2.5 $CaCl_2$, 2.5 KCl, or low-Ca rACSF – 1.3 $MgSO_4$, 1 $CaCl_2$, 2.5 KCl. Electrophysiological data were acquired by Multiclamp 700A (Molecular Devices) and a National Instruments acquisition interface. The data were filtered at 3 kHz, digitized at 10 kHz and collected by Igor Pro 6.0 (Wavemetrics). Input resistance was analyzed online.

Neuron classification

Neurons were classified as pyramidal neurons according to pyramidal-like soma shape, the presence of an apical dendrite and spines visible after Alexa filling reconstruction as well as according to regular spiking in response to 500 ms suprathreshold intracellular current injection (Figure 1A-C).

In an initial series of experiments using wild-type mice, where neuron subtypes were not genetically labeled, inhibitory neurons were identified by 1) their non-pyramidal soma shape, 2) a lack of dendritic spines viewed at 40x magnification after filling with Alexa, and 3) characteristic physiological spike trains elicited during 500 ms suprathreshold intracellular current steps. LTS/Sst cell firing during current steps demonstrated spike-rate adaptation, and the AHP after the first action potential was more negative than the last AHP during the current step [S3, S4]. In contrast, FS/PV cells were identified by a non-adapting firing patterns and AHP magnitudes that were uniform throughout a given current step. In experiments where Sst neurons could be identified using fluorescent reporter gene expression, i.e. in SstCre-Ai14 or SstCre- Ai35D mice, the same firing criteria described above for wild-type Sst cells was also used to verify cell identity. Apparent Sst cells identified by fluorescent reporter expression that exhibited FS firing patterns were excluded from further analysis [S5]. Non-LTS/Sst or FS/PV inhibitory interneurons, approximately 1/3 of the population of supragranular inhibitory neurons [S6] frequently displayed delayed action potentials during current injection, similar to what has been described for NGF cells [S7, S8, S9].

Spontaneous firing frequency was calculated by counting action potentials over 4-5 minutes of recording in different ACSFs. V_{rest} was never adjusted. In cells where activity was compared across different recording solutions, mACSF and rACSF were applied in random order.

Connectivity analysis

Cells were maintained at their normal resting potential, i.e., current was not injected to maintain a specific resting membrane potential during the course of the experiment. EPSP properties were evaluated for cells only when V_{rest} of the post-synaptic cell was <-55 mV and R_i was >200 mW. Each cell was alternatively assigned as the trigger cell and a series of 10 pulses (1000 pA, 4-5 ms duration) at 20 Hz were delivered across 20 separate trials (0.1 Hz). Because recurrent activity in network Upstates made EPSP identification difficult, only responses collected during Downstates were evaluated.

Pharmacology

The $GABA_b$ receptor agonist baclofen (10 μM, Sigma) or antagonist CGP 55845 (1μM, Tocris) were bath applied for at least 10 minutes before data acquisition to assess drug effect for 20 trails of the 10-pulse train. Typically, either baclofen or CGP was applied, although in a subset of experiments both drugs were applied in sequence, where baclofen was followed by CGP, since the effects of CGP did not wash out and the order could not be reversed.

Virus injection and optical stimulation

Sst-IRES-Cre mice, aged between postnatal days 13-15, were injected *i.p.* with Ketamine/Xylazine mixture (80 mg/kg body weight for Ketamine and 13 mg/kg body weight for Xylazine) and immobilized in a stereotaxic frame. A small craniotomy was made over the barrel cortex, typically 0.8 mm posterior to Bregma and 3.8 mm lateral to the midline. Adeno-associated virus carrying a fusion gene for ArchT under CRE control (rAAV1/flex-ArchT-GFP, UNC Vector Core) was delivered using a glass micropipette (tip diameter 10-20 μm) attached to a picospritzer microinjector (WPI). Virus was injected every 50μm starting at ≈1mm depth until the top of L2, ~100μm from the pia. Experiments were conducted 7-10 days after virus injection. In a second approach to deliver Arch to Sst neurons, Sst-IRES -Cre homozygous mice were crossed with homozygous Ai35D mice carrying a floxed Arch-GFP transgene. Offspring from this cross were heterozygous for both Sst-Cre and Ai35. EPSP results from Sst silencing in virally-transduced or transgenic mice were indistinguishable and were combined for analysis.

Prior to photostimulation, slices were incubated in the dark, and visible light was introduced only during cell-targeting for patching. Unless indicated, electrophysiological recordings were carried out under darkness. Photo stimulation was produced by a light-emitting diode (white LED with 535 nm 41002 HQ filter, set to maximum range, Prizmatix, Israel) and delivered through a 40x water-immersion objective. Spontaneous activity of fluorescently labeled Sst neurons was recorded and a 1 s illumination pulse was delivered to determine the effect on V_{rest} and spontaneous firing rate. Magnitude of Sst hyperpolarization was calculated at the start of the light pulse. To enable reduction in GABAb activity (since receptor activation can persist for 100s of ms) [S10] and assess the effect of silencing on EPSP amplitude, Sst silencing was initiated 500 ms prior to the 10 pulse presynaptic train. Trials were delivered at 0.1 Hz, and at least 20 baseline, light OFF trials were collected before initiating light ON trials. CGP was applied for at least 10 minutes before assessing EPSP properties, and stimuli were not delivered during drug wash-on.

Data analysis

Evoked EPSPs were calculated using responses from 10 trials stimulus trials, where trials initiated during UP states were excluded from analysis because responses were difficult to isolate from background activity in the sweep. Because L2 pyramidal neurons rarely fire more than a single spike and almost never at frequencies exceeding 20 Hz, we considered responses to the first presynaptic spike to be most representative of synaptic function as it might occur *in vivo*. Thus, measurements of amplitude and failure rates are plotted for the EPSP evoked by the first artificial pulse only, except for heat-map figures where amplitudes for all EPSPs are shown. For all heat-map figures of EPSP responses across the entire 10-pulse train, maximum amplitude (red) was set for the individual connection plotted. PPR was calculated as the amplitude of the 2nd/1st EPSP. Because EPSP amplitudes could vary more than 10-fold, EPSP amplitudes were normalized to the baseline value for each connection in order to compare light ON and light OFF trials. Normalization was also applied to compare failure rates during light ON and OFF trials. Population data are presented as mean ± SEM. Statistical significance was defined as $p<0.05$ using a two-tailed unequal variance t-test. When two conditions were compared within the same cell a two-tailed paired t-test was used. When more than two conditions for the same cell were compared (i.e., across mACSF, rACSF, and rACSF with 1 mM Ca^{2+}), an ANOVA was performed with Tukey-Kramer test for post-hoc comparisons.

Supplemental References

S1. Finnerty, G.T., Roberts, L.S., and Connors, B.W. (1999). Sensory experience modifies the short-term dynamics of neocortical synapses. Nature 400, 367-371.

S2. Maier, N., Tejero-Cantero, A., Dorrn, A.L., Winterer, J., Beed, P.S., Morris, G., Kempter, R., Poulet, J.F., Leibold, C., and Schmitz, D. Coherent phasic excitation during hippocampal ripples. Neuron 72, 137-152.

S3. Beierlein, M., Gibson, J.R., and Connors, B.W. (2003). Two dynamically distinct inhibitory networks in layer 4 of the neocortex. Journal of neurophysiology 90, 2987-3000.

S4. Fanselow, E.E., Richardson, K.A., and Connors, B.W. (2008). Selective, state-dependent activation of somatostatin-expressing inhibitory interneurons in mouse neocortex. Journal of neurophysiology 100, 2640-2652.

S5. Hu, H., Cavendish, J.Z., and Agmon, A. Not all that glitters is gold: off-target recombination in the somatostatin-IRES-Cre mouse line labels a subset of fast-spiking interneurons. Frontiers in neural circuits 7, 195.

S6. Lee, S., Kruglikov, I., Huang, Z.J., Fishell, G., and Rudy, B. A disinhibitory circuit mediates motor integration in the somatosensory cortex. Nature neuroscience 16, 1662-1670.

S7. Olah, S., Fule, M., Komlosi, G., Varga, C., Baldi, R., Barzo, P., and Tamas, G. (2009). Regulation of cortical microcircuits by unitary GABA-mediated volume transmission. Nature 461, 1278-1281.

S8. Tamas, G., Lorincz, A., Simon, A., and Szabadics, J. (2003). Identified sources and targets of slow inhibition in the neocortex. Science (New York, N.Y 299, 1902-1905.

S9. Kawaguchi, Y., and Kubota, Y. (1997). GABAergic cell subtypes and their synaptic connections in rat frontal cortex. Cereb Cortex 7, 476-486.

S10. Thomson, A.M., and Destexhe, A. (1999). Dual intracellular recordings and computational models of slow inhibitory postsynaptic potentials in rat neocortical and hippocampal slices. Neuroscience 92, 1193-1215.